Electronic Supplementary Information

Charge Separation in Nanostep Structured Perovskite-Type Photocatalyst Induced by Successive Surface Heterojunctions

Xiaoyan Cai,[ab†] *Liang Mao,*[a†] *Junying Zhang,*[*a] *Mingshan Zhu,*[b] *Mamoru Fujitsuka,*[b] *and Tetsuro Majima*[*b]

[a] Key Laboratory of Micro-nano Measurement, Manipulation and Physics (Ministry of Education), Department of Physics, Beihang University, Beijing 100191, P.R. China

[b] The Institute of Scientific and Industrial Research (SANKEN), Osaka University, Mihogaoka 8-1, Ibaraki, Osaka 567-0047, Japan

[†] These authors contributed equally to this work

[*]Corresponding authors: zjy@buaa.edu.cn (J. Zhang); majima@sanken.osaka-u.ac.jp (T. Majima)

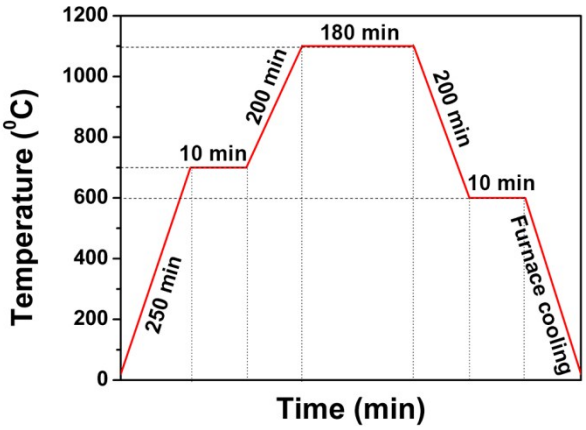

Scheme S1 Temperature-time plot of the heating and cooling process for preparation of LTO NSP.

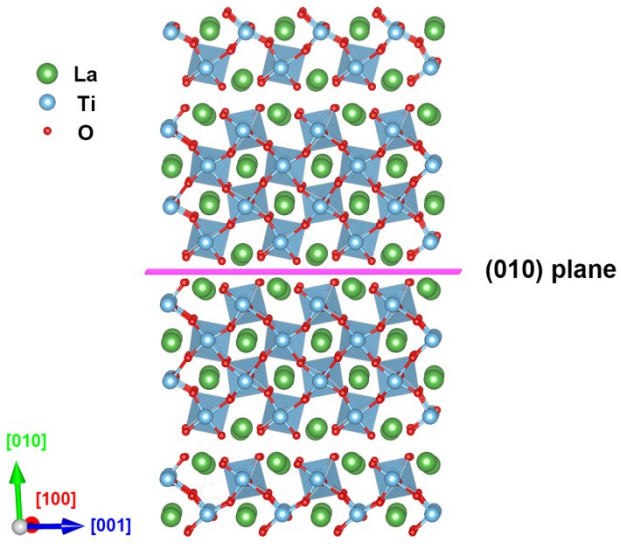

Fig. S1 Perovskite structure of LTO. Due to the unbounded oxygen atoms, the perovskite LTO are readily formed into two-dimensional plate structure and thus exposing the O-terminational inactive (010) surfaces.

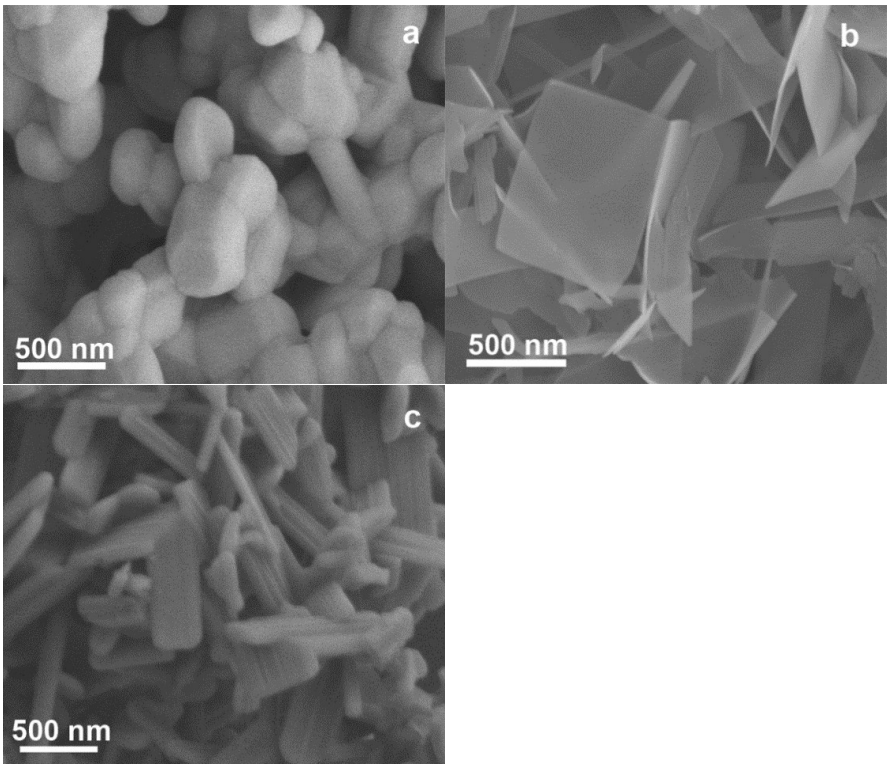

Fig. S2 SEM images of LTO NP (a), LTO NS (b), and LTO NSP (c).

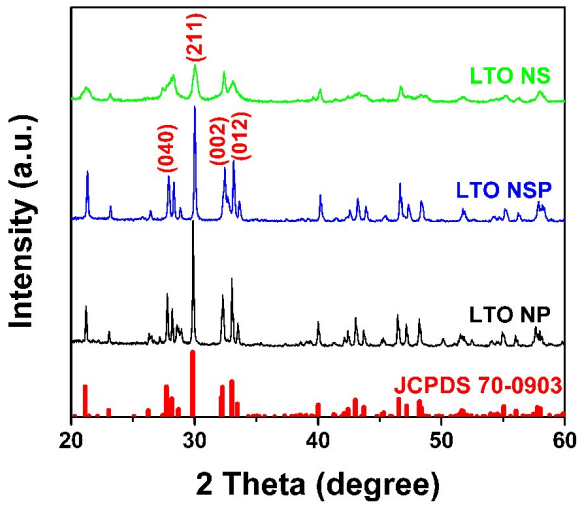

Fig. S3 XRD patterns of the different LTO samples.

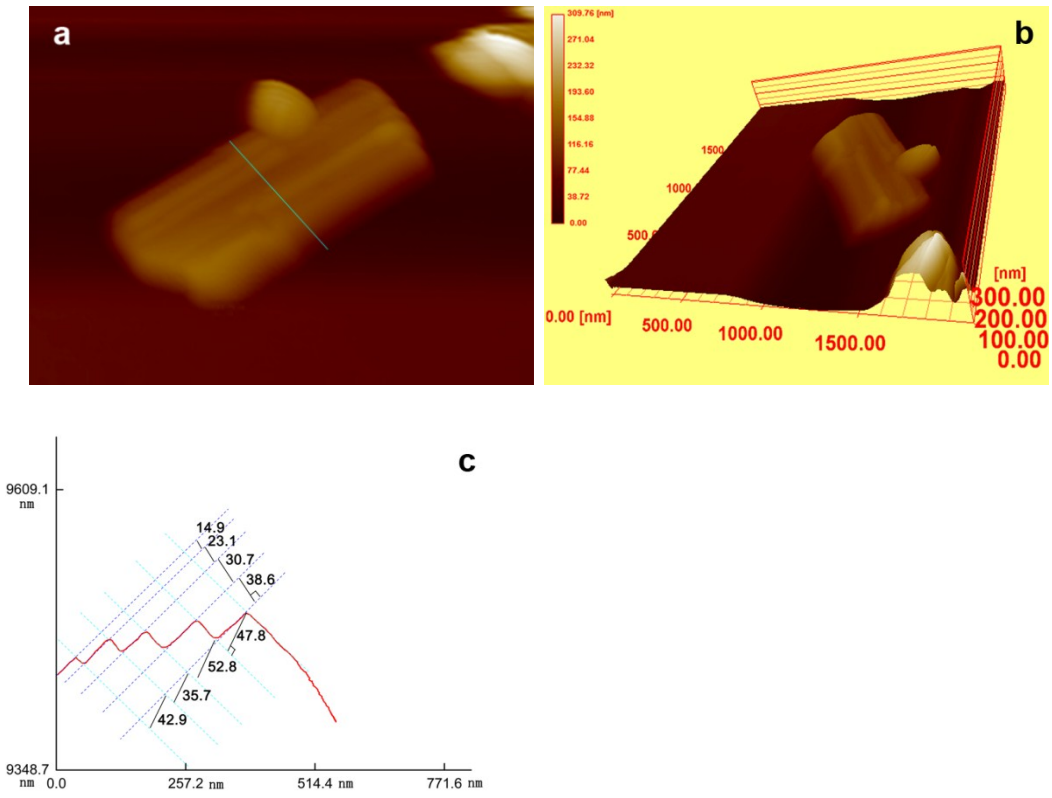

Fig. S4 AFM images of LTO NSP in 2D (a) and 3D (b) perspective, and the corresponding height profile analysis (c).

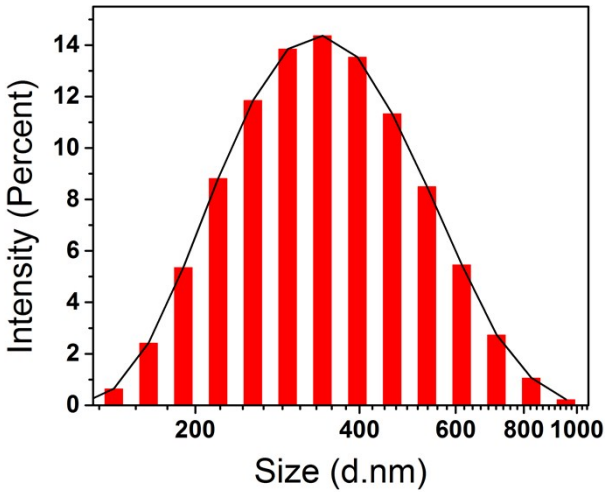

Fig. S5 Particle size distribution of LTO NSP.

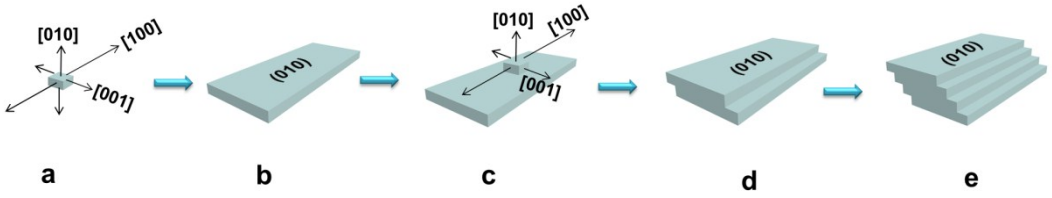

Fig. S6 Schematic representation of processes involved in LTO NSP crystal growth.

According to the model of layer growth provided by Kossel,[S1,S2] we envision the crystal surface as made of cubic units which form layers of monoatomic height, growing along [100], [001], and [010] direction (Fig. S6a). The growth velocities of the LTO crystals in different directions are [100] > [001] > [010], suggesting that the (010) facets grow most slowly compared to other facets. Limited by step (or edge), a (010) facet exposed multi-atomic LTO layer is formed firstly (Fig. S6b). Then, a new step will be formed by the nucleation of an island of monolayer height (or 2D nucleus) on the crystal surface (Fig. S6c). Step and terrace coexisting growth occurs when the nucleation is too fast for the step to cover the whole crystal surface. The variations of surface topography happen when the secondary 2D nuclei form on different location of the (010) surface. Those nuclei concentrated on the (010) surface will spread and coalesce to form step-like structure.

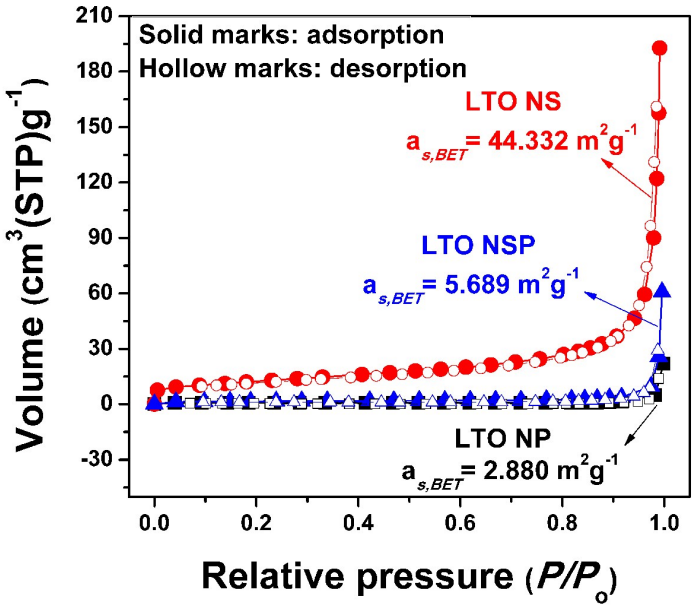

Fig. S7 N_2 adsorption-desorption isotherms of the different LTO samples.

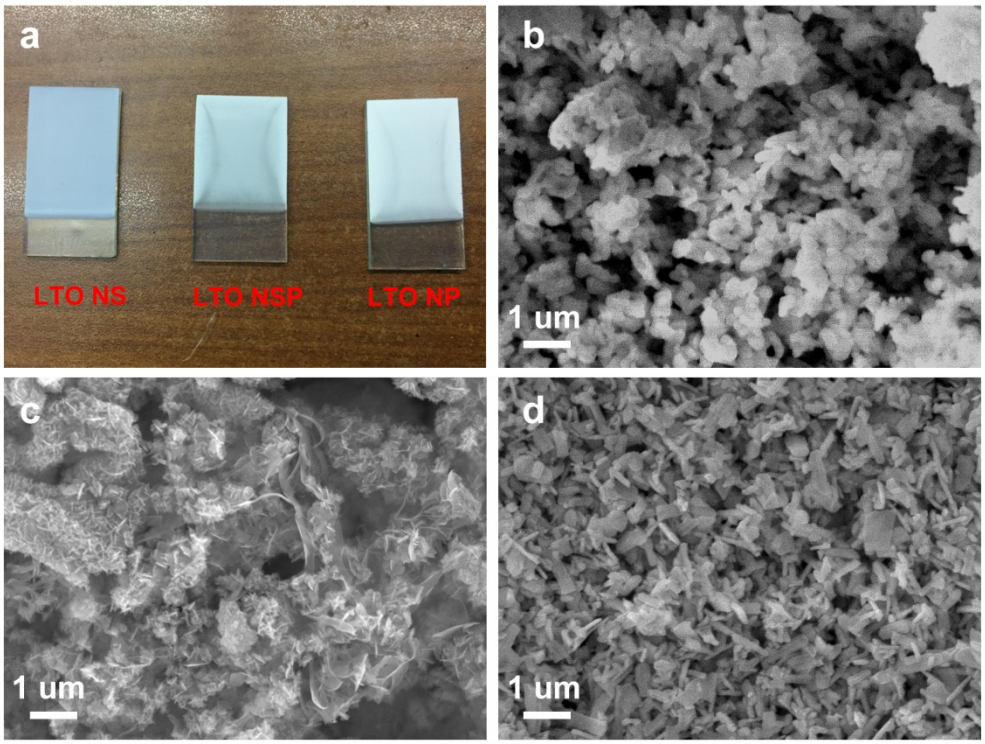

Fig. S8 Photographs of the different LTO electrodes (a). SEM images of LTO NP (a), LTO NS (b), and LTO NSP (c) film electrode surfaces.

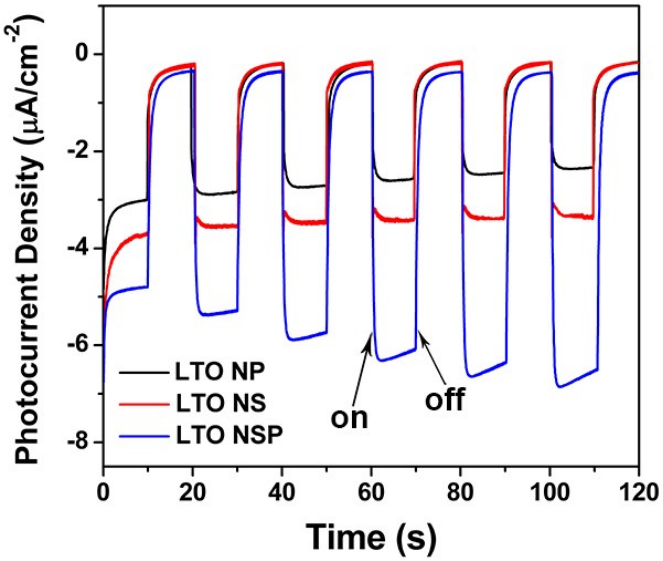

Fig. S9 Time-dependent photocurrent density response of the different LTO electrodes.

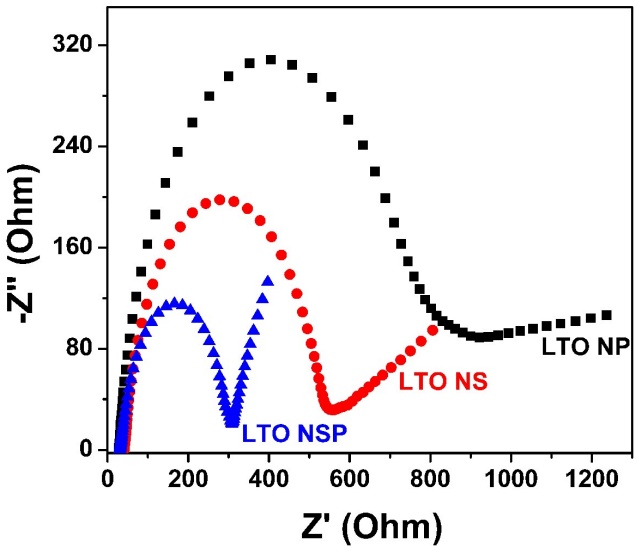

Fig. S10 Electrochemical impedance spectroscopy (EIS) Nynquist plots of the different LTO electrodes.

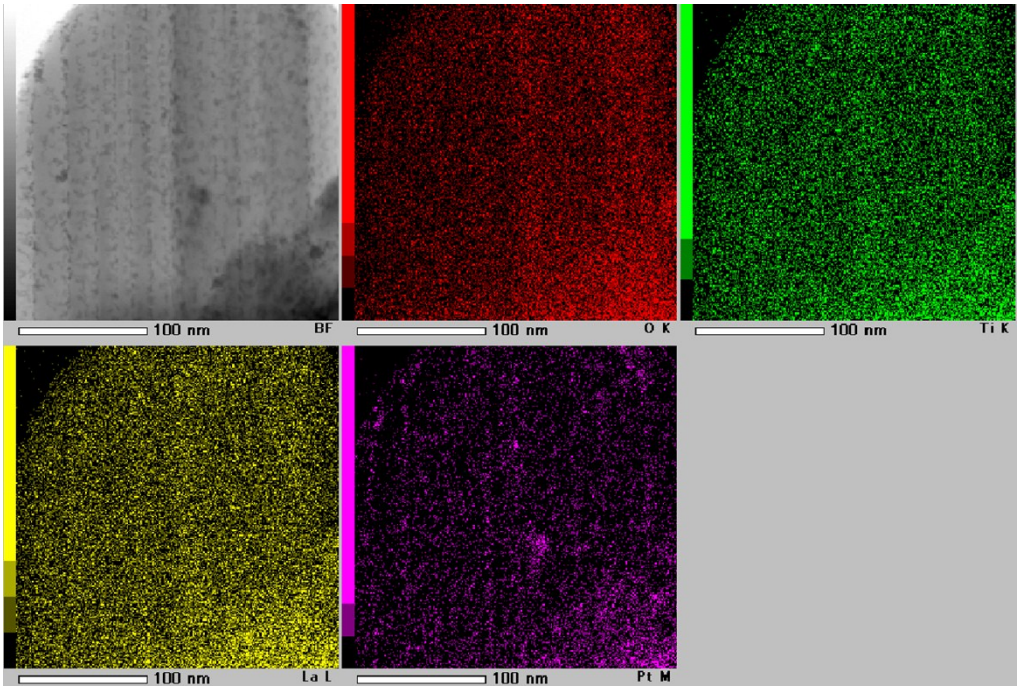

Fig. S11 STEM-EDS elemental mapping images of Pt selectively deposited LTO NSP.

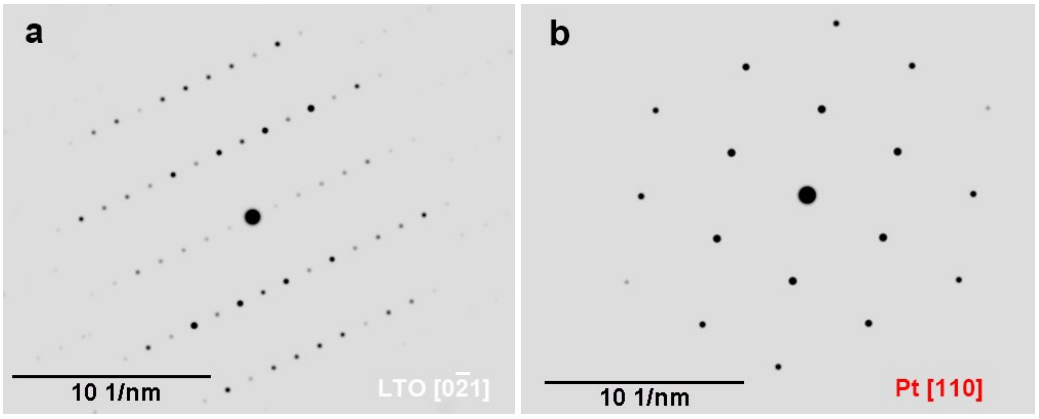

Fig. S12 Simulative SAED patterns of single-crystal LTO along [0-21] zone axis (a) and Pt along [110] zone axis (b).

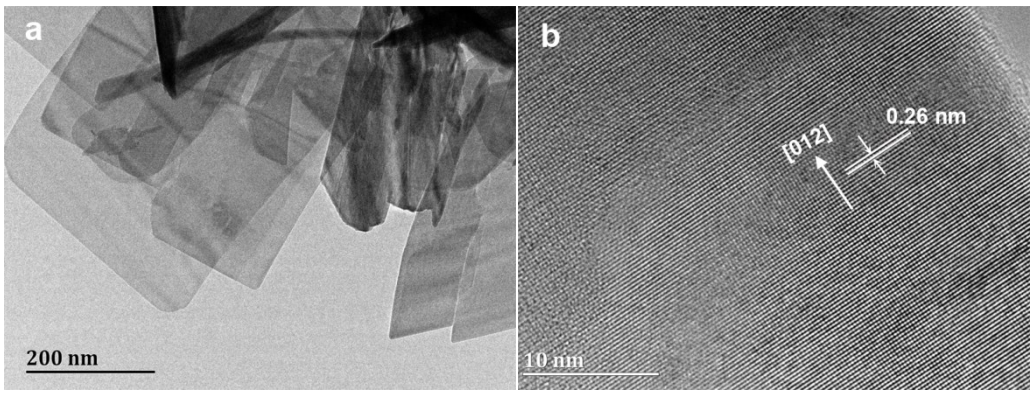

Fig. S13 TEM image (a) and HRTEM image (b) of LTO NS.

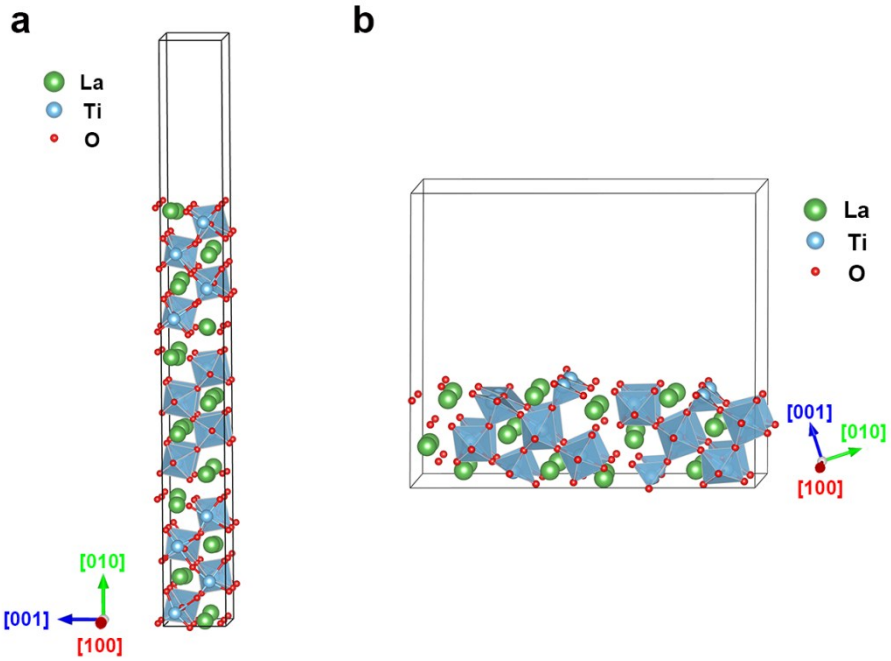

Fig. S14 Relaxed geometries for the (010) (a) and (012) (b) surfaces of LTO based on a 132-atom slab model. The vacuum region was set to the same thickness of 15 Å.

Our surface models were based on slabs comprised of 44×3 atoms with a vacuum region of the same thickness for both (010) and (012) facets as shown in Fig. S14. Each surface was constructed such that the correct stoichiometry was satisfied on both sides of the slab. Geometry relaxations were performed with the mid-layers fixed. The surface energy γ was computed using:[34]

$$\gamma = (E_{slab}\text{-}nE_{bulk})/2A$$

Where E_{slab} is the total energy of the slab and E_{bulk} is the total energy of the bulk per unit cell, n is the number of bulk unit cells contained in the slab, and A is the surface area of each side of the slab. Here, n = 3 and A = a×b. The computational results are revealed in Table S1.

Table S1 Surface energies of ideal surfaces of (010) and (012) facets.

	Bulk	(010)	(012)
E	-388.176	-1161.62	-1117.20
a (nm)		0.5546	0.7716
b (nm)		0.7800	2.661
A (nm^2)		0.43258800	2.0532276
$E_{surface}$ ($eV \cdot nm^{-2}$)		3.361165821	11.52526880
$E_{surface}$ ($J \cdot m^{-2}$)		0.5384587640	1.846348062

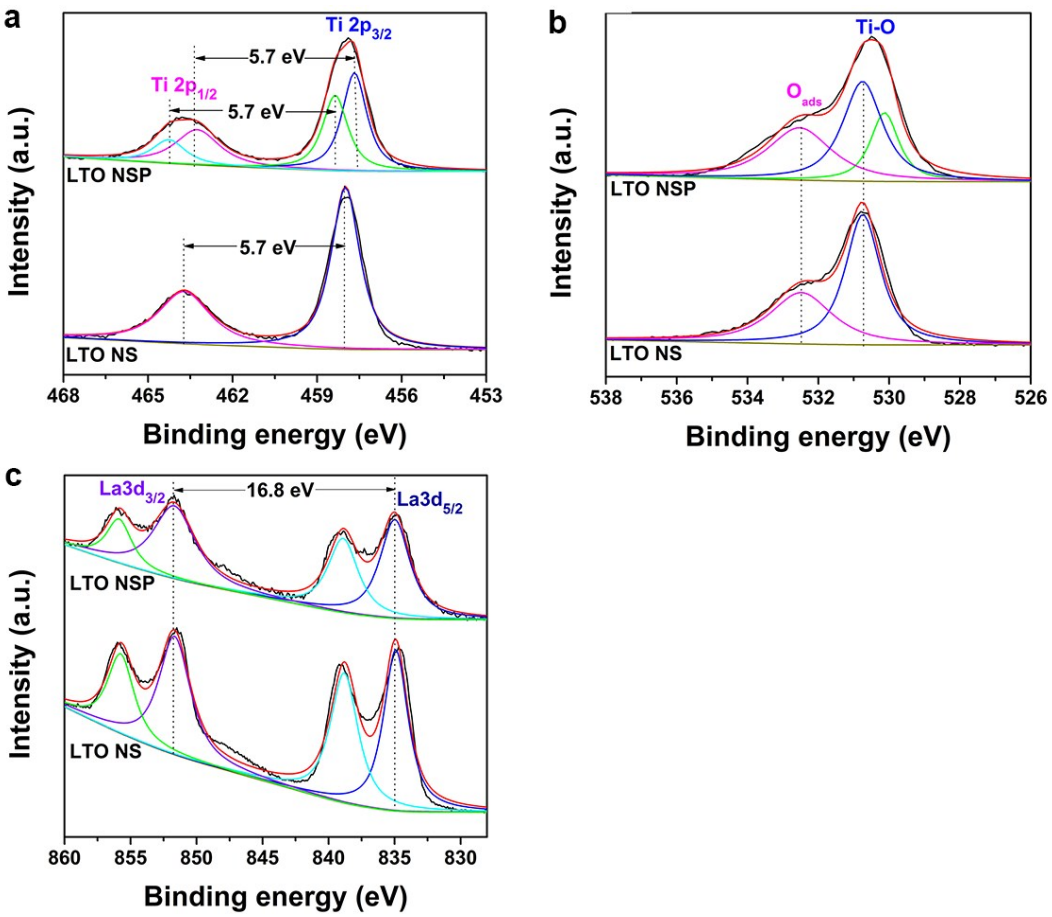

Fig. S15 High-resolution XPS spectra of Ti 2p (a), O 1s (b), and La 3d (c) of the different samples.

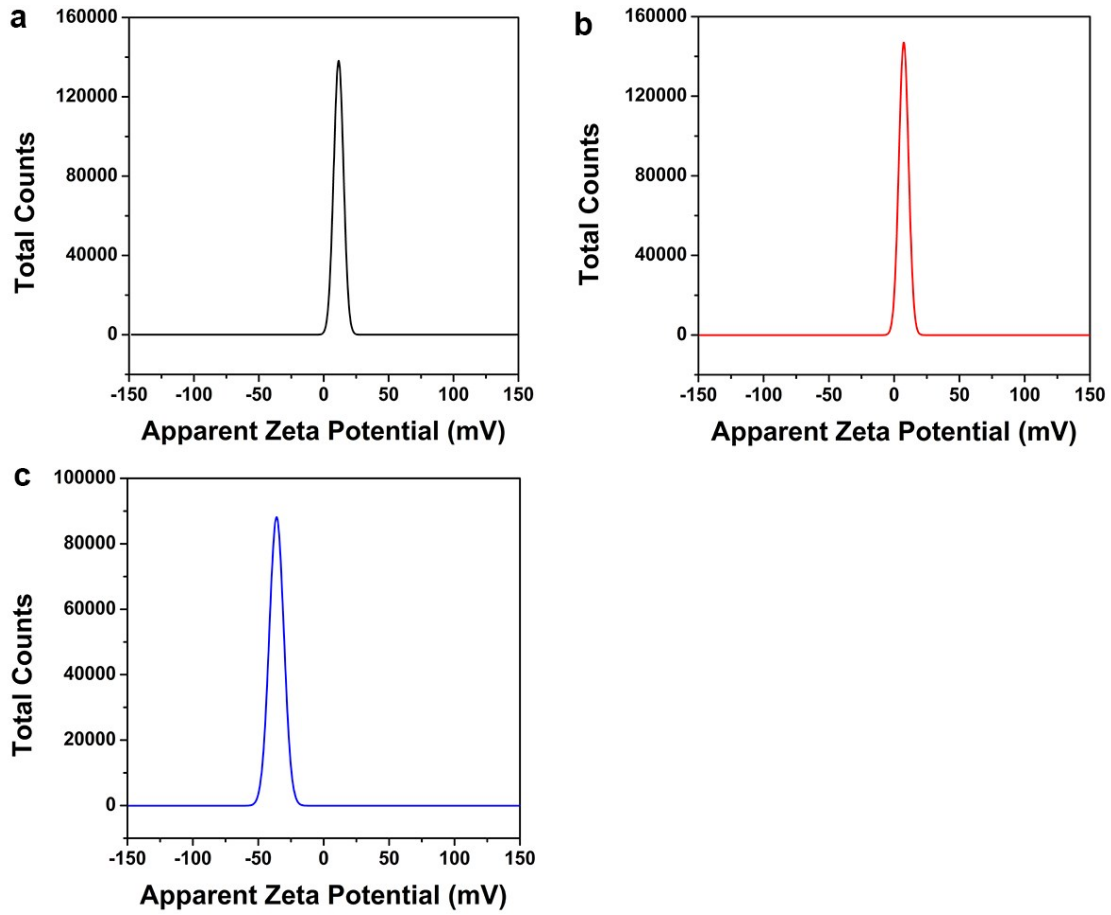

Fig. S16 Zeta potential of LTO NP (a), NS (b), and NSP (c) suspended in aqueous solution at pH = 7.2.

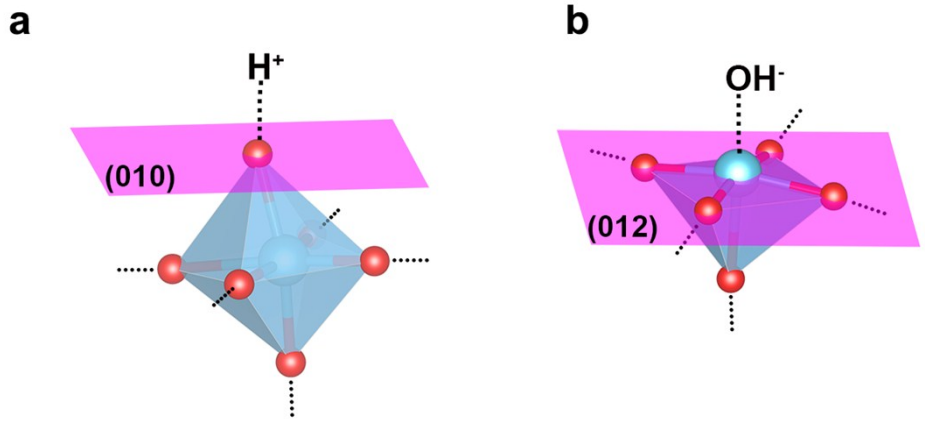

Fig. S17 Assumed surface structure of (010) facet (a) and (012) facet (b) in aqueous solution at pH = 7.2.

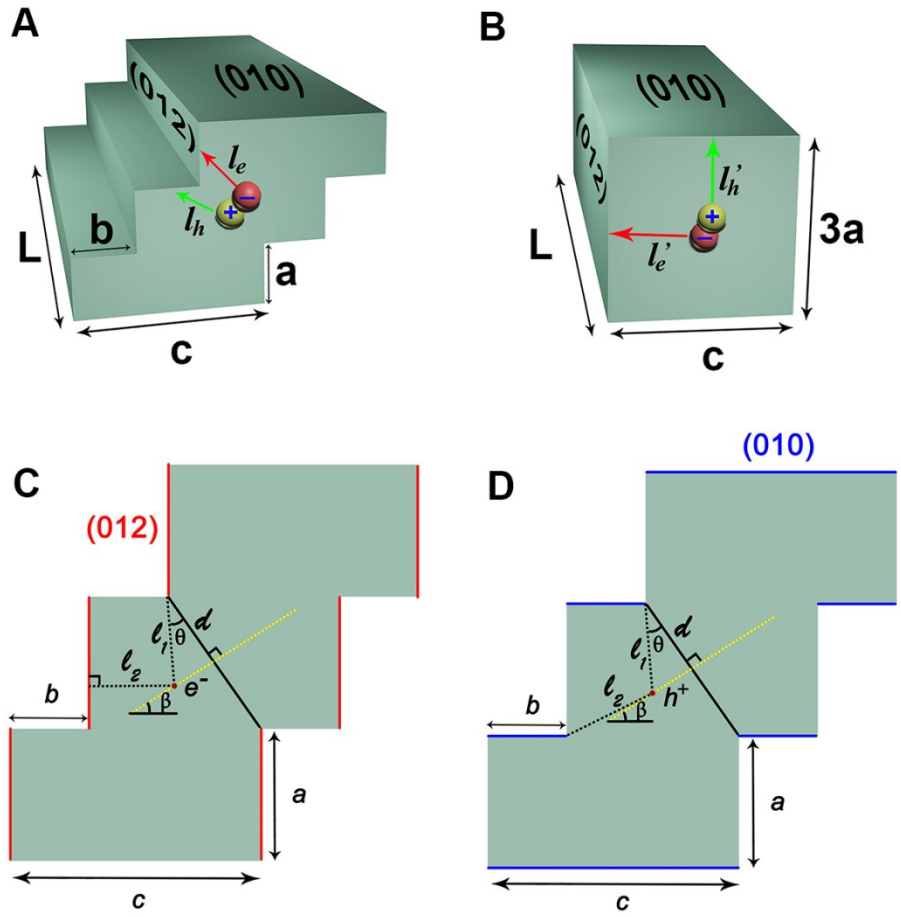

Fig. S18 Models of charge carrier migration processes in successive surface heterojunctions (A) and conventional surface heterojunction (B). Analysis of electron (C) and hole (D) transport distance in successive surface heterojunctions.

In Fig. S18C, the electrons transport distance (l_e) from excited site to nearby (012) surfaces are maximized when $l_1 = l_2$, which can be calculated as follows:

$$l_e = l_1 = l_2$$

$$l_1 = d/cos(\theta)$$

$$l_2 = \frac{C}{2} - d * \tan(\theta) * \cos(\beta)$$

$$\tan(\beta) = \frac{c - 2b}{a}$$

In Fig. S18D, the holes transport distance (l_h) from excited site to nearby (010) surfaces are maximized when $l_1 = l_2$, which can be calculated as follows:

$$l_h = l_1 = l_2$$

$$l_1 = d/cos(\theta)$$

$$l_2 = \sqrt{\left(\frac{a}{2} - d * \tan(\theta) * \cos(\beta)\right)^2 + \left(\frac{C}{2} - d * \tan(\theta) * \cos(\beta)\right)^2}$$

$$\tan(\beta) = \frac{c - 2b}{a}$$

Where l_1 and l_2 are electrons (or holes) transport distance from the excited sites to the two nearby (012) (or (010)) surfaces. The independent parameter a = 26.8 nm, b = 44.8 nm, c =85.3 nm, and L= 350 nm are obtained from SEM and AFM analysis. The calculation results are summarized in Table S2.

Table S2 Transport distance of electron and hole in different models.

Model	**l_e (nm)**	**l_h (nm)**
Successive surface heterojunctions	30.8	32.1
Conventional surface heterojunction	42.7	67.2

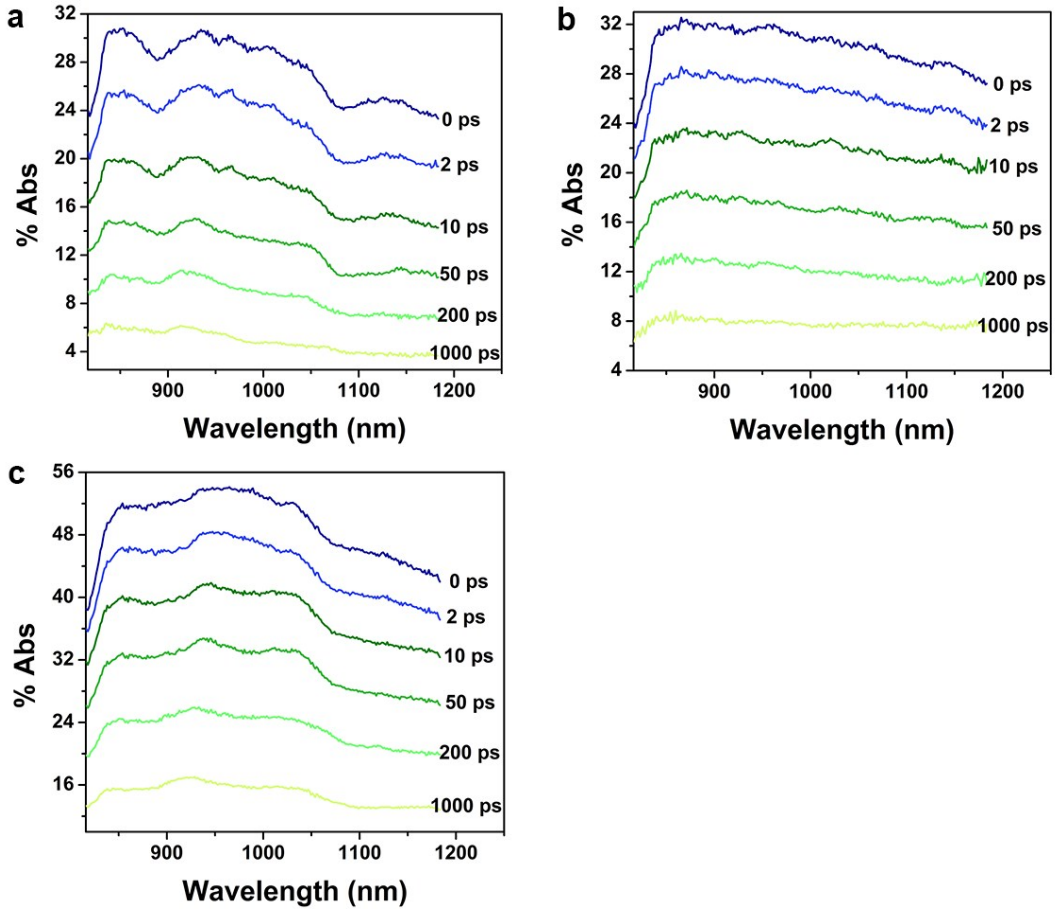

Fig. S19 Time-resolved diffuse reflectance spectra of LTO NP (a), NS (b), and NSP (c).

Reference

S1 W. Kossel, *Annal. Phys.*, 1934, **21**, 457-480.

S2 P. Cubillas, M. W. Anderson, Zeolites and Catalysis, Synthesis, Reactions and Applications, J. Čejka, A. Corma, S. Zones, Eds., *Wiley-VCH*, 2010, pp 1-55.